Journal of Geomine (2025), 3(4), 225-238
DOI: 10.22077/jgm.2026.11029.1076

Engineering geological modeling and stability assessment of the Niasar waterfall slope using advanced nonation techniques

Hasnain Haider[1*], Enayatallah Emami Meybodi[2]

Recived: 2026 Apr. 26, Revised: 2026 May 17, Accepted: 2026 May 30, Published: 2026 Jul. 07

ABSTRACT

Naisar, a small town near Kashan in Iran's Isfahan province, is renowned for its historical pavilion, locally known as the 'Khooshk.' This significant structure is endangered by an unstable karstified rock mass beneath it. The rock, primarily travertine carbonate, is extensively characterized by vugs, cracks, and fractures. Impurities, including sand, clay, gypsum, and intermixed marl (predominantly in the uppermost sections), further compromise its structural integrity. The site, encompassing the pavilion and a nearby waterfall, is a popular tourist destination attracting both national and international visitors. The precarious foundation and slope conditions present a substantial future risk, with a high potential for loss of life and property damage if the instability is not mitigated. This study analyzes the slope using the numerical modeling software UDEC 4.0. After identifying potential failure mechanisms, an advanced micro- and macro-zonation of the rock mass was conducted. This zonation aims to precisely delineate stable and unstable areas, establishing a clear and actionable framework for geotechnical engineering interventions. Any proposed mitigation strategies must carefully balance the imperative to preserve the site's original aesthetic and structural authenticity with the practical need for cost-effectiveness. The findings and detailed zonation map from this study are designed to meet both essential criteria, facilitating a targeted and sensitive approach to stabilizing this valuable historical and natural landmark.

KEYWORDS

Numerical modeling, micro and macro zoning, slope stabilization, engineering geology mapping, geotechnical assessment

I. INTRODUCTION

Niasar is a small town located approximately 23 km from Kashan, renowned for its spring and attracting numerous visitors annually, including both Iranian nationals and international tourists interested in its natural and historical sites. Karst, a geological process involving the dissolution of bedrock and the formation of underground drainage systems, is not exclusively associated with limestone but also occurs in other carbonate rocks (Waltham et al., 2005). Schlumberger (2011) provided case studies in which the digenetic effects like karstification created very large scale vuggs which had increased the permeability of certain zones within carbonate reservoirs. The rock on which the Niasar Pavilion (Kooshk) is built is highly permeable and pours travertine limestone mass having impurities like marl, clay, sand and shale layers between it. Karstic cavities are spaces created by dissolution, overlaid onto the fracture network (Meybodi and Hussain, 2022). Studies emphasize that both geological controls and triggering factors must be considered together when assessing slope instability and failure potential (Ehsan et al., 2025). The rock in this area is highly porous and permeable, exhibiting significant karstification due to the underground water source feeding the Niasar spring. This pervasive underground water has facilitated the formation of numerous natural caves through dissolution processes. Among these, the approximately 1 km long Raees Cave, located beneath the Niasar Pavilion (Kooshk), is particularly noteworthy. Furthermore, weathering processes, exacerbated by rainfall, snowfall, vegetation, and human activities, have increased the instability of the exposed rock. In the past, some rock fragments have broken off and fallen near the village. There is a considerable future risk that similar rock failures could occur, potentially leading to the complete destruction of the historical Niasar Pavilion (Kooshk). Recent studies highlight that the precise characterization of discontinuity geometry and the methods used for data acquisition significantly influence rockfall susceptibility assessments (Lukačić et al., 2024). The area presents a considerable risk, necessitating precautions to ensure the safety of both local residents and visitors. However, a primary concern when applying engineering methods must be the preservation of the rock's inherent beauty and unaltered appearance.

[1]Department of and Mining & Metallurgical Engineering Yazd University, Yazd, Iran, [2]Department of Geology, Yazd University, Yazd Iran
✉ H. Haider: haider.cca@gmail.com

Karstification contributes to the instability of rock slopes, both natural and man-made, by forming dissolution cavities and widening existing joints within the rock mass (Meybodi et al., 2022). The study aimed to utilize the UDEC 4.0 numerical modeling technique to analyze the behavior of the Niasar slope under various conditions with and without hydraulic pressure, and with and without horizontal acceleration. Following the numerical modeling, zonation was performed by creating an engineering geology map. This map identifies areas experiencing significant stress, indicating a need for stabilization through engineering techniques. Given the highly karstified nature of the rock, parameters for modeling the slope were assumed based on results from slake durability and Schmidt hammer field tests. The values obtained from these two tests corroborate the highly karstified nature of the rock and its rapid weathering due to constant exposure.

II. Geology of the Study Area

The geology of the area was studied using the 1:100,000 geological map of Kashan, Iran. A section of this map is shown below, extracted from the 1:100,000 Kashan geological map. The geology of the area is somewhat complex. It features Pliocene-age travertine limestone, which is surrounded on the northwest side by an igneous body of Eocene age. This igneous body consists of dark grey to reddish-grey pyroclastic rocks and lavas with varying compositions and textures, interbedded with some nummulite-bearing volcanosedimentary rocks and limestone, represented by the symbol EV6 on the geological map. Above and below this rock body are dark grey shale, green marl, sandy marl limestone, and reefal limestone of the Qom Formation, which is Oligocene in age and represented by OMq on the map. On the NW side above the Qom Formation, there is another Oligocene outcrop consisting of altered limestone with marl and shale, represented on the map as OM ml q. On the NE side of the study area, the Qom Formation extends further. The southwest and southeast sides are bordered by green-grey siliceous tuff, tuff breccia, shale, marl, limestone, and pyroclastic rocks, locally including meta-siliceous tuff, all of Eocene age. The geological map of the study area is shown above in Fig. 1 (Aghanabati, 2004).

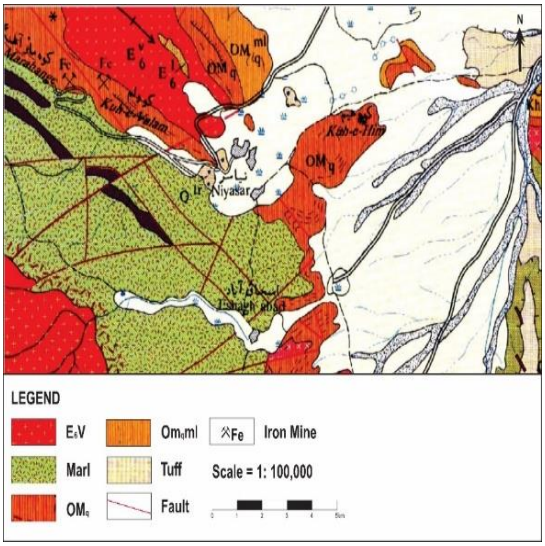

Fig. 1. Geological map of study area taken from kashan 1:100000 map

III. Previous Incident of Rock Fall

Approximately thirty years ago, a moderate-magnitude seismic event triggered a significant rockfall on the Niasar slope. Two large rock blocks detached from the slope and descended into the populated area. While fortuitously no casualties were reported, the earthquake exacerbated existing geological conditions. Specifically, it widened a pre-existing tension crack, estimated to be 30 meters deep and 1 to 1.5 meters wide, located near the slope's crest. This event, along with the subsequent development of new fissures and voids within the slope's rock wall, heightened concerns among government and local authorities regarding the stability of this historical site and the safety of the Niasar village population. The incident underscored the urgent need for intervention to preserve the area for both tourism and local residents.

Fig. 2. The figure displays caves formed by the weathering and erosion of impurities and soft materials, with evidence of clay and sand presence observed.

Fig. 3. Approximately 30 years ago, an earthquake caused these two massive stones to separate from the wall and fall into the inhabited area below.

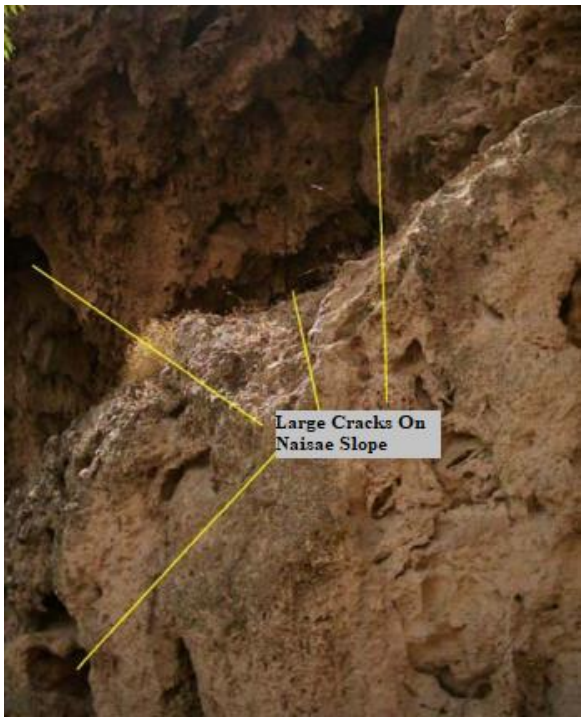

Fig. 4. Development of new cracks and voids after a seismic episode

IV. ROCK STRENGTH DETERMINATION USING SCHMIDT HAMMER

The rock strength was evaluated using a Schmidt hammer. Tests were performed at multiple locations around the waterfall, pavilion, and the staircase connecting them. Field observations indicated generally weak rock characteristics throughout most of the tested areas. This weakness is primarily attributed to the presence of marl and gypsum interspersed with limestone and travertine within the rock mass. Schmidt hammer rebound values ranged from 10 to 15, indicating low rock strength at nearly all tested sites. Similar low values were recorded inside the cave, further confirming the overall rock weakness. These findings classify the rock in the study area as a weak rock type, likely due to its mineralogical composition.

Fig. 5. Schmidt Hammer test

V. SLAKE DURABILITY TEST

In the engineering laboratory at Yazd University, slake durability tests were conducted on various rock samples over multiple cycles to assess their durability. The following results were obtained:

Table 1. Schmidt hammer test results

Schmidt hammer test		
S.No	Marly Travertine (MPA)	Travertine Partially Strong (MPA)
1	10	12
2	11	13
3	10	11
4	12	14
5	10	15
6	11	12
7	11	15
8	12	14
9	10	12
10	12	11
11	10	15
12	10	14
13	11	13
14	10	13
15	13	12
16	10	11
17	11	15
18	12	14
19	10	13
20	10	13

Fig. 6. Slake Durability test for rock

Total weight of 10 rock pieces' oven dried W1= 274 grams

Total weight of 10 rock pieces after 2 cycles and oven dried W2=178 grams

Using formula:

SDI= W2/W1 * 100= 178/274 *100= 64.9%

Based on the Standard Test Index, the rock is classified as having medium durability.

VI. Slope Modeling of Niasar using UDEC 4.0

1. Dry slope model – This model represents the Niasar slope without influence of pore pressure or groundwater flow, allowing for an evaluation of its inherent stability under dry conditions.

2. A hydraulic slope model – This model simulates the slope under hydraulic conditions, incorporating the effects of water infiltration, pore water pressure, and seepage forces to analyze their roles in destabilizing the slope.

VII. Model Construction

The solid model was developed in Surpac using elevation data from an AutoCAD file, which provided precise topographical information. This allowed for the accurate representation of the slope's geometry. The constructed model was then imported into UDEC, a numerical modeling software commonly used for analyzing rock mechanics and slope stability. The wall has a vertical height of 60 meters, extending from the base (toe) of the slope up to the foundation of the historical structure located at the crest.The lateral boundaries in the x-direction are fixed (horizontal displacement is set to zero). The upper boundary and the slope surface are considered free boundaries. The bottom boundary of the model is fixed in both the x and y directions (horizontal and vertical displacements at the bottom boundary are set to zero). The wall profile features a non-uniform slope angle, transitioning from a shallow 20° at the base to a vertical orientation (90°) near the upper portion adjacent to the historical building.

For highly karstified rock masses, the appropriate approach is to treat them as very weak, highly heterogeneous rock mass conditions. Due to the extensive karstification, it is nearly impossible to obtain core samples for geotechnical testing or to apply rock classification methods such as RMR or RQD. For these highly karstified rocks, which are also considered very weak according to Hoek and Brown (1997), the following parameter values are typically used: cohesion of 0.3 MPa, elastic modulus of 1 GPa, Poisson's ratio of 0.3, friction angle of 25 degrees, UCS of 3 MPa, and rock mass modulus of 0.5 GPa. These values are perfect for the highly karstified or weak rocks (Marinos and Hoek, 2000). The chosen parameters are not intended to represent pristine intact rock but rather a highly degraded karstified rock mass under realistic field conditions. They are adopted as conservative design inputs to reflect the weak mechanical behavior of the slope material and the combined effects of discontinuities, groundwater, weathering, and surface water.

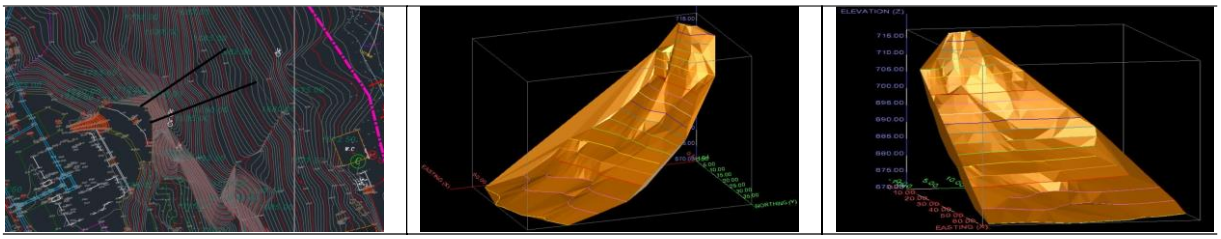

Fig. 7. Cross section and solid diagram of the sections that are taken for the modeling

VIII. NUMERICAL MODEL OF SECTION 1 WITHOUT CRACKS

The simulation, excluding the effects of cracks, reveals that the slope is stable under the applied load and the presence of a tension crack alone, as evidenced by the near-zero displacement and absence of failure. This highlights the critical role that voids and cracks play in compromising slope integrity.

A. Numerical model of section 1 with cracks

Section 1 indicates that the presence of voids and cracks under real conditions, combined with the applied load on the Niasr waterfall slope, increases the potential for slope failure. Greater displacement is observed when cracks and voids are present within the slope mass.

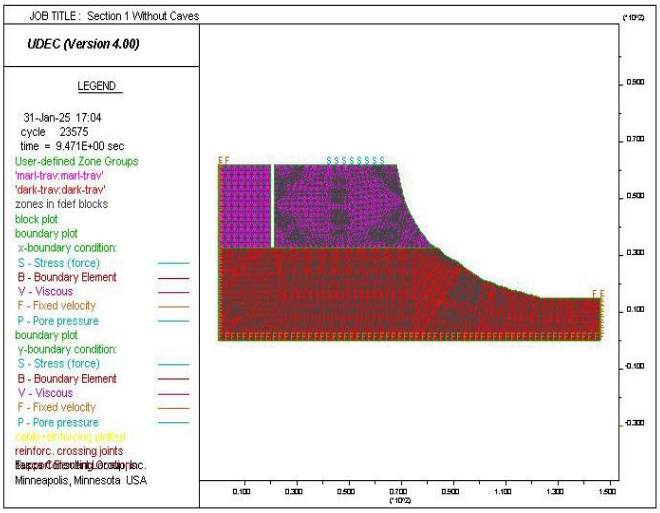

Fig. 8. This model, referencing Section 1 (the scenario without cracks), visualizes the parameters used, showing negligible displacement and no observed failure after the given load cycles.

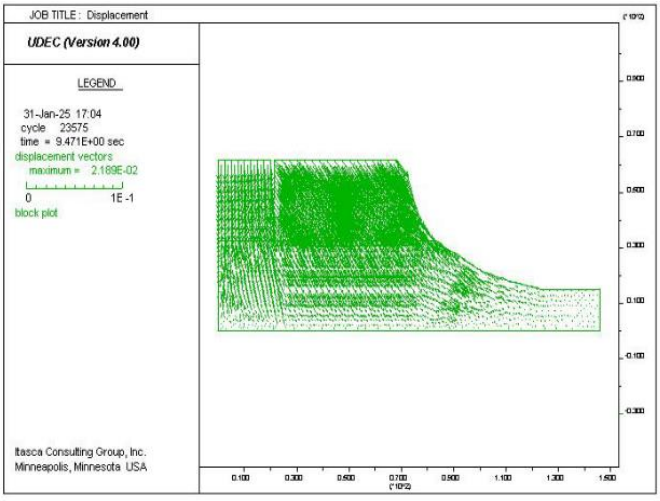

Fig. 9. The displacement model illustrates the direction of block movement under forces applied from above and from the right via the tension crack. In this scenario, no visible or significant movement has been observed.

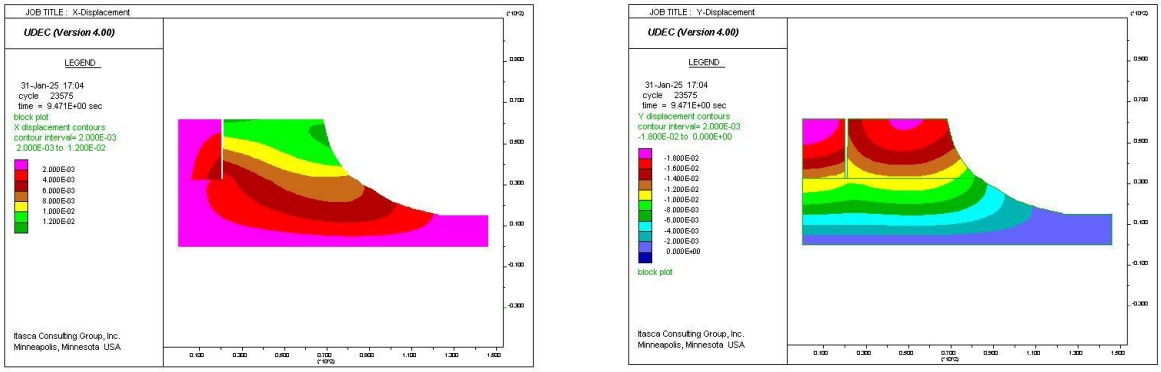

Fig. 10. According to the X and Y displacement model, when cracks and voids are absent, the displacement is negligible or entirely absent, even under applied load conditions

The plastic model shows that just beneath the Niasr building, there is a possibility of a new tension crack to develop. Tensile failure may occur at the points marked in the figure and observed within the slope.

The model illustrates the maximum and minimum stress distribution under loading applied from both the top and the tension crack. The results show stress concentration at a single location, just beneath the Niasr building and near the pre-existing cracks.

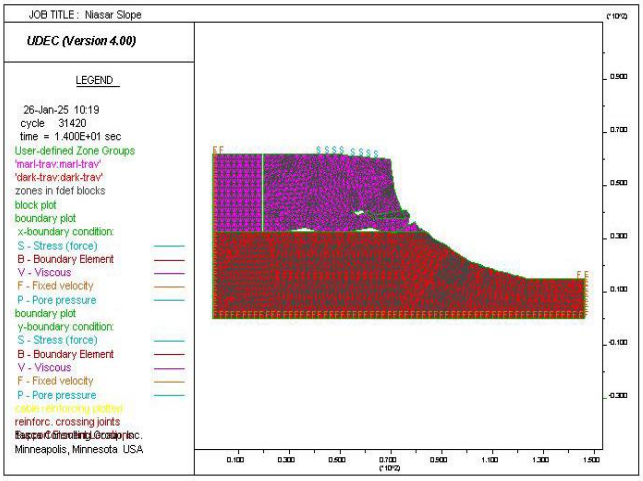

Fig. 11. This model corresponds to Section 1, which contains cracks. The parameters used in the analysis are clearly indicated in the model diagram. The cracks and applied load caused the slope to fail.

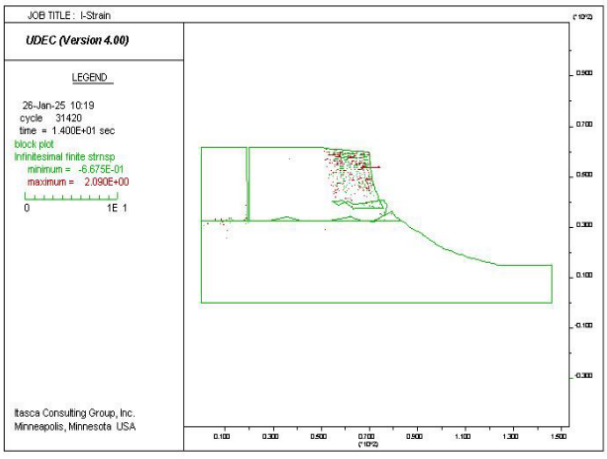

Fig. 12. This model depicts the maximum strain occurring at the slope's tip, directly attributable to the load from the Niasr building. The analysis shows this load is causing strain and movement originating from the slope's apex.

Displacment Diagram with Horizontal Accelration 3

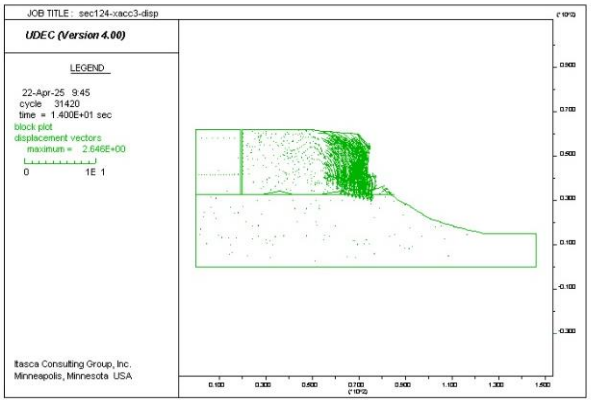

Displacement Diagram with Horizontal Acdelration 0

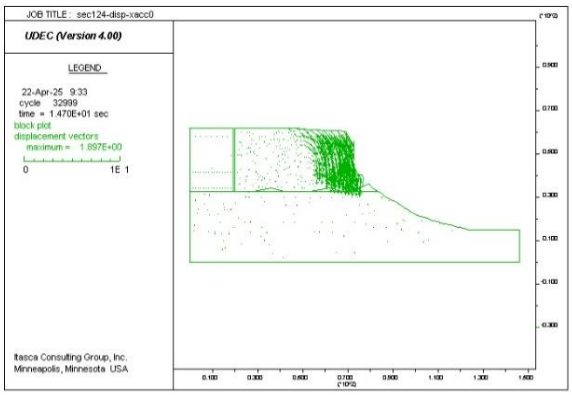

Fig 13. The displacement model indicates that the inclusion of horizontal acceleration results in a higher displacement rate than in the case without horizontal acceleration.

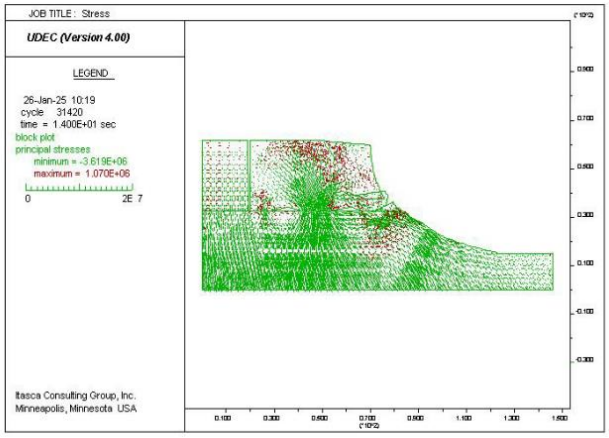

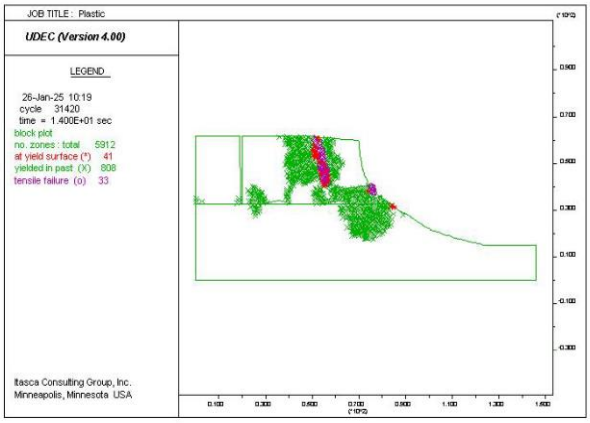

Fig. 14. Plastic and stress response model of section 1 naisar slope

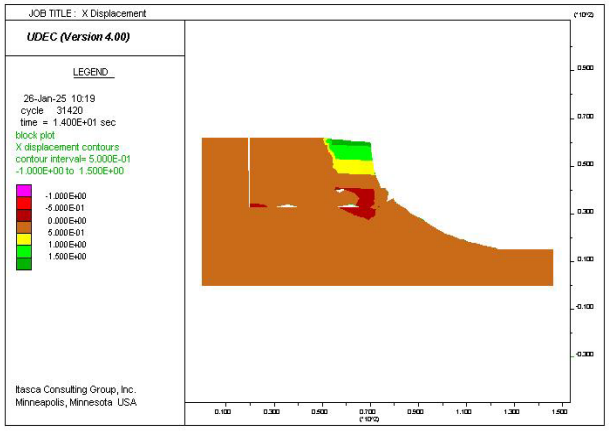

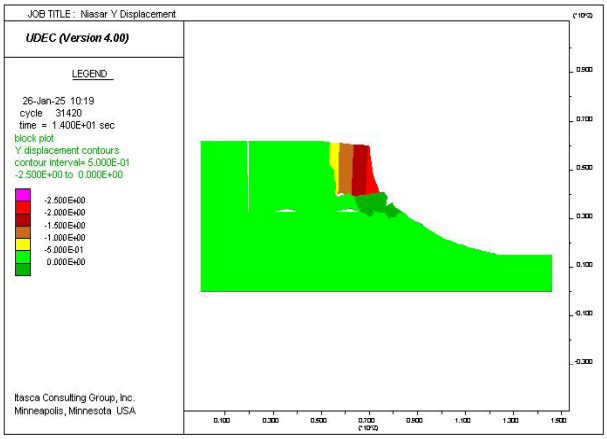

Fig. 15. The X and Y displacement model indicates that the combined presence of cracks, voids, and the vertical load of the Niasar building caused displacement, which moved the block from the tip and pushed the slope toward failure.

B. Numerical model of section 2 without crack

For Section 2, the simulation without cracks shows that the slope remains stable under load, exhibiting near-zero displacement and no failure. However, displacement occurs only at the unstable tip, where the applied load causes it to slide downward.

C. Numerical model of section 2 with cracks

Section 2 shows that the presence of voids and cracks under real conditions, combined with the applied load from the Niasar waterfall structure, increases the likelihood of slope failure. Larger displacements are observed when cracks and voids exist within the slope mass. In this section, the slope toe is unstable, resulting in a very high probability of failure. As the slope fails and

moves due to the tension cracks and applied load, the entire slope becomes a hazardous zone.

The maximum strain values occur directly beneath the Niasar building and in areas where tension cracks are present. This concentration of strain indicates that the slope is deforming toward the pre-fractured zone, ultimately triggering the failure mechanism.

The plastic model indicates that the development of a yield surface directly beneath the Niasar building may initiate tensile failure. These resulting movements can lead to collapse in areas adjacent to cracks and void zones.

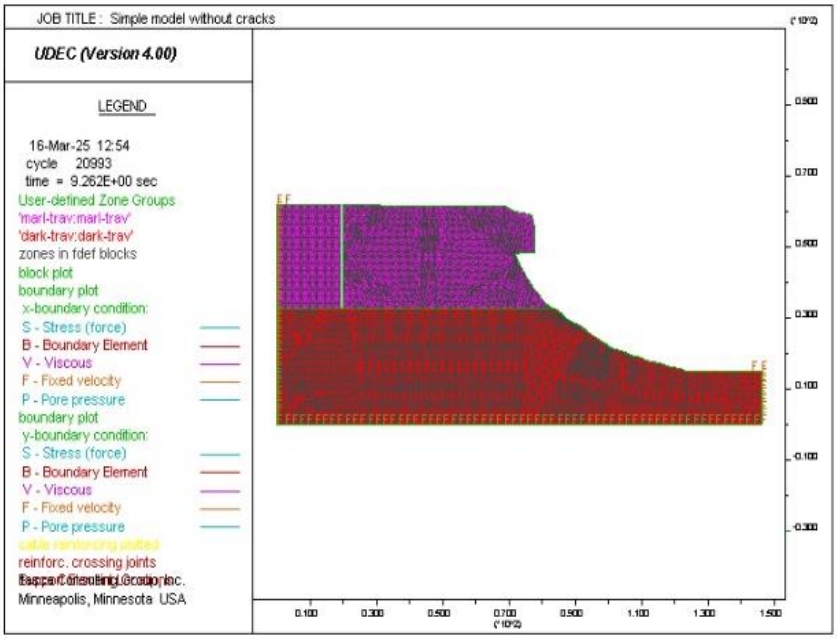

Fig. 16. Section 2 of the model, which is free of cracks, illustrates the parameters employed. The results show negligible displacement and no observed failure after the specified load cycles.

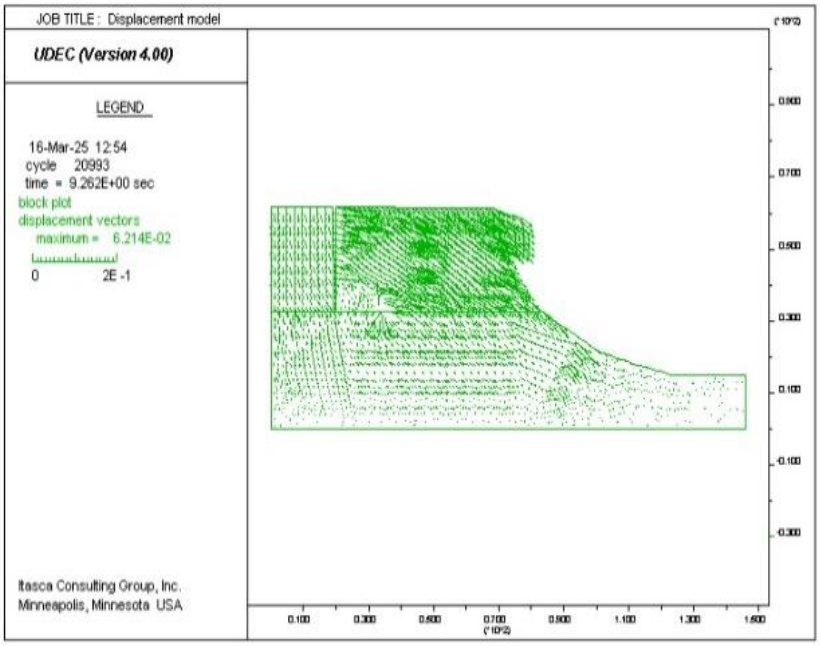

Fig. 17. The displacement model for Section 2 illustrates downward movement of the entire tip of the slope when the load is applied. This displacement is attributed to forces originating from above and the presence of a tension crack.

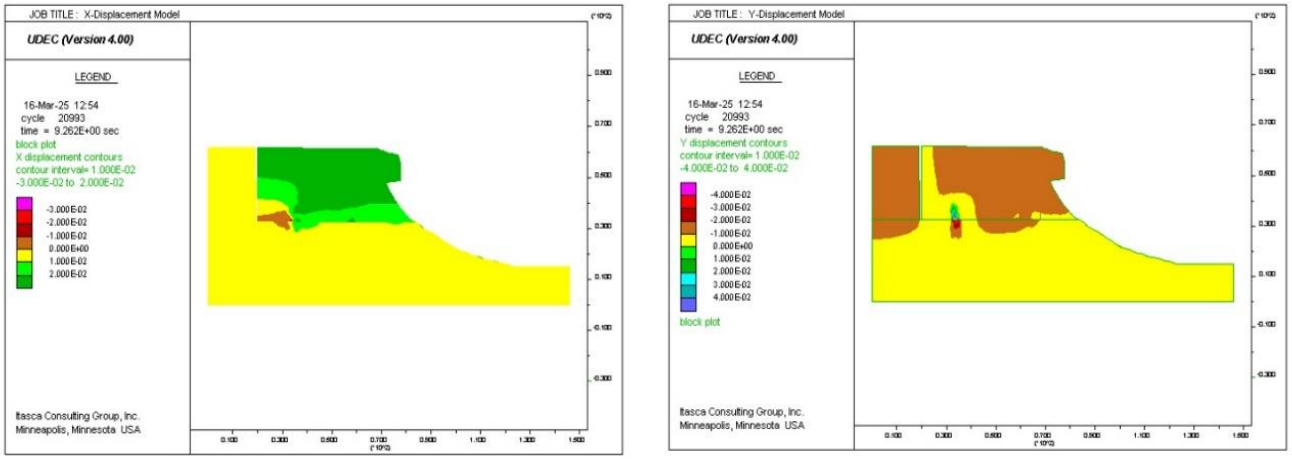

Fig. 18. The X and Y displacement model diagram of Section 2 shows that, under these typical conditions, the slope still moves even when voids are neglected. This movement is due to instability at the slope tip and the applied load from the Niasar Khoosk building.

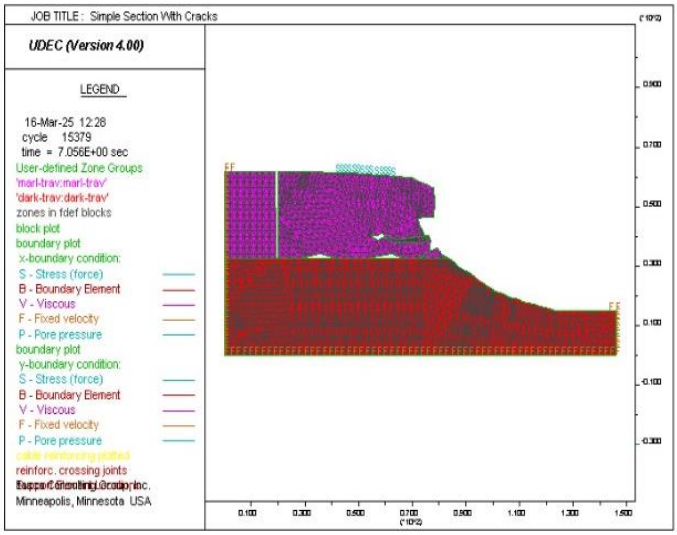

Fig. 19. Referring to Section 2, the model diagram illustrates that cracks and the applied load induce sliding and movement at the slope's tip.

Displacment Diagram with Horizontal Accelration 3

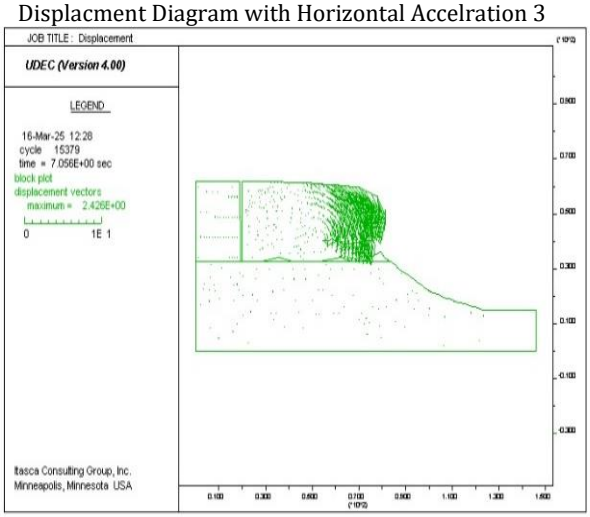

Displacment Diagram with Horizontal Accelration 0

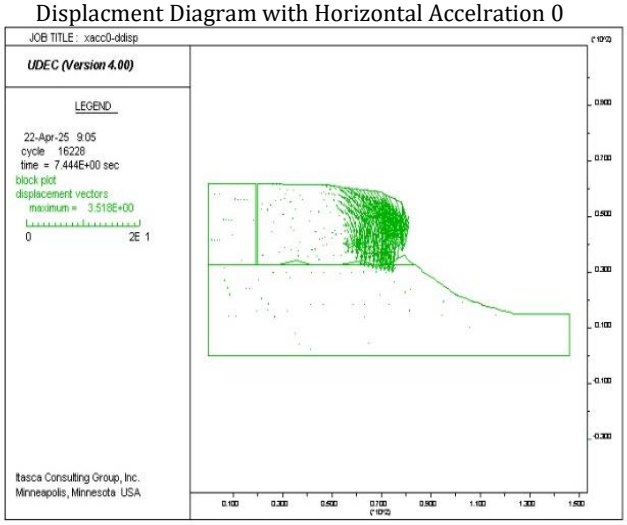

Fig. 20. Displacement model diagram showing the slope behavior with and without horizontal acceleration

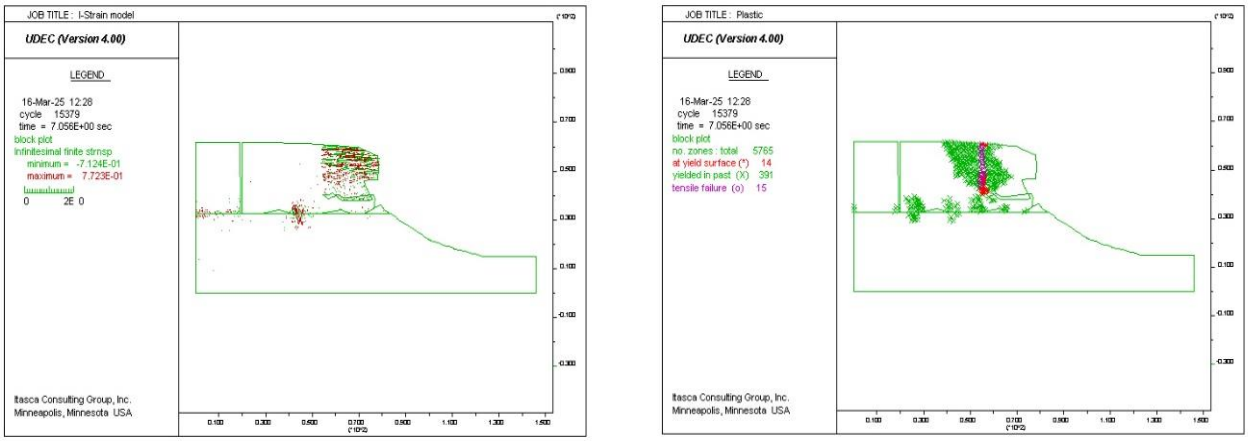

Fig. 21. Both the I-Strain and Stress models highlight zones susceptible to new tension crack formation and potential slope failures.

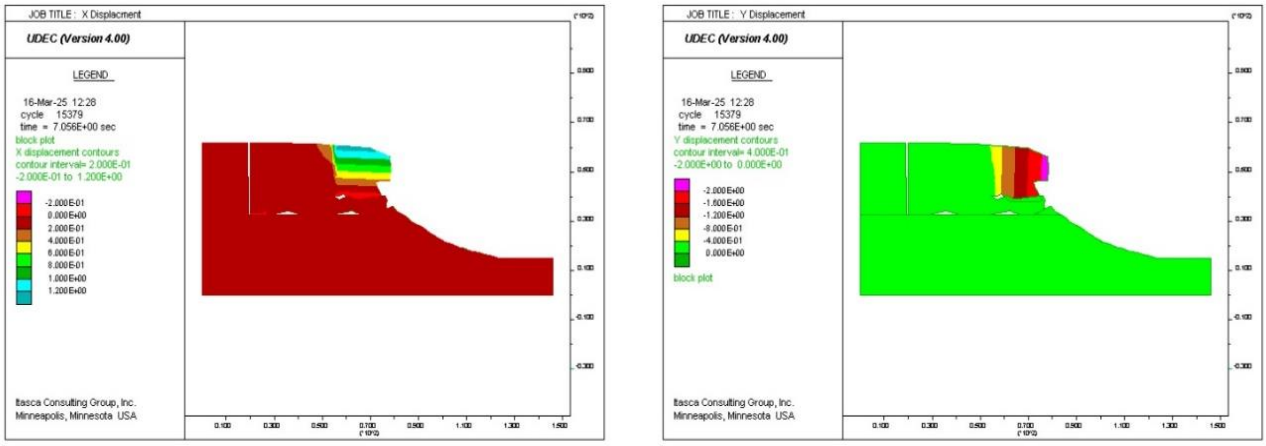

Fig. 22. The X and Y displacement model shows that cracks, voids, and the Niasar building's vertical load combined to displace the block, pushing the slope towards failure.

IX. TOTAL DISPLACEMENT GRAPH FOR ALL SECTION WITHOUT CRACKS

This analysis highlights the critical role of structural discontinuities in slope stability. In the absence of cracks or karstic voids, the slope remains inherently stable, and stabilization measures may not be necessary. However, when fractures are present, appropriate reinforcement techniques become essential to prevent slope failure and ensure long-term stability.

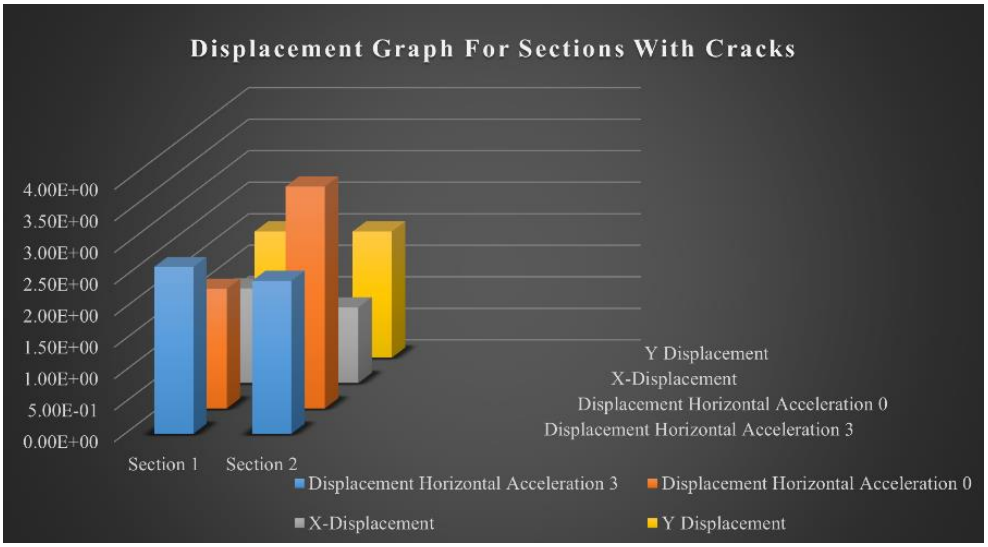

Fig. 23. Total displacement graph of the sections with cracks, with and without horizontal acceleration

X. NUMERICAL MODELING OF WET SECTION (HYDRULIC MODEL)

The hydraulic model shows the effect of water pressure on slope stability. When pore water pressure increases in the cracks, it weakens the internal resistance of the slope. This causes flow movement both at the base and through the tension cracks. Consequently, the slope begins to deform and displace, potentially resulting in failure from its original position. Hydrogeological conditions and seepage processes in karst systems significantly influence slope failure by altering stress conditions and eroding unstable zones (Li et al., 2025).

A. Impact of Cracks and Karstification on Slope Stability

The numerical analysis results highlight the critical role of structural discontinuities in slope stability. A fundamental difference emerged between two simulated scenarios: the model representing an intact, non-karstified rock mass showed no significant displacement under load, indicating high inherent stability in the absence of major weaknesses. Conversely, the model incorporating realistic geological conditions, specifically pre-existing cracks and karstified limestone features, predicted noticeable slope movement. These discontinuities serve as planes of weakness, drastically reducing the overall shear strength of the rock mass and facilitating deformation. This vulnerability is further amplified by the presence of water; the hydraulic model, which simulates pore water pressure within these fractures, exhibited an even greater magnitude of displacement. The hydrological pressure effectively reduces the normal stress acting on fracture surfaces, diminishing frictional resistance and promoting slip along the discontinuities. This confirms that water acts not merely as a passive agent but as an active driver of instability, transforming existing weak zones into pathways for progressive failure. Consequently, the combined effect of geological discontinuities and hydrological forcing renders the slope highly susceptible to failure under applied loads.

B. Instability Potential in Structural Section

Section with High Instability Potential:

Plan Area: 125.71 m^2, Height: 15 meters, Approximate Volume: 125.71 m^2 * 15 m = 1885 m^3

Description: This section is highly prone to instability due to its design and structure.

Potential Instability in the Small Pavilion Section

Plan Area: 1931 m^2, Height: Approx. 30 meters, Approximate Volume: 1931 m^2 * 30 m = 57930 m^3

Description: The small pavilion section is prone to instability, primarily caused by the tensile crack at the end of the structure, which detaches from the rear section.

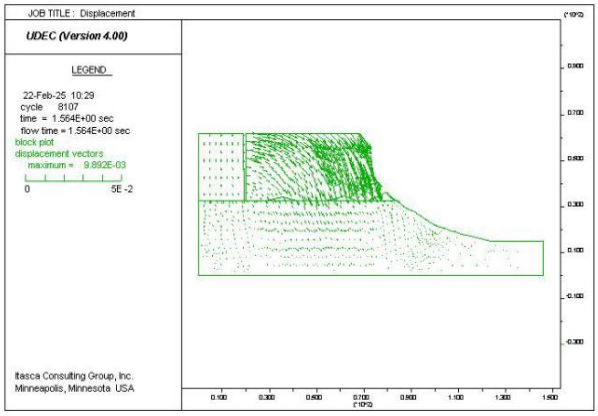

Fig. 24. The displacement model under hydraulic conditions indicates that upon application of pore pressure, the slope begins to move from its tip, subsequent to the influence of the Niasar building as depicted in the model diagram

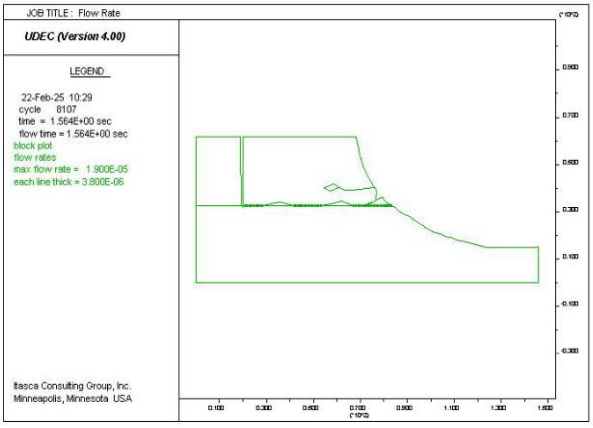

Fig. 25. The flow-rate model, driven by the force exerted by water within the cracks, shows flow occurring both at the toe and through the tension crack, which causes the slope to fail and displace from its original position

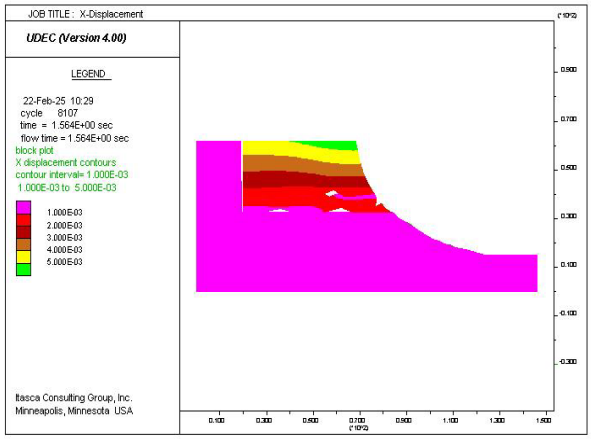

Fig. 26. The X-dispalcement shows that in the pore pressure condition the slope started to move from the tip and this displacement is high near the tip and as the depth increase it decreases

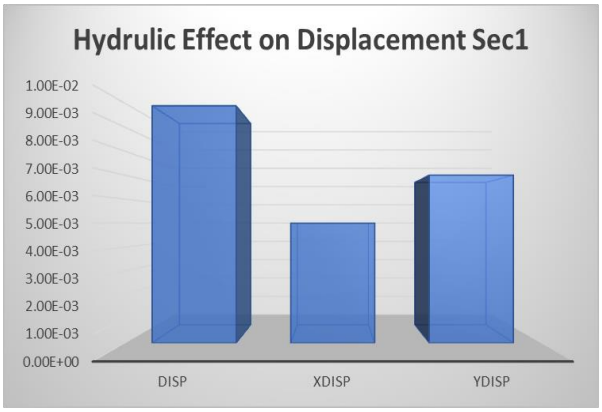

Fig. 27. Total Displacement graph of Hydraulic Model

C. Potential Failure Due to Load-Induced Cracking

Section with Potential Failure:

Volume of Affected Area: Approx. 18,000 m^3

Description: The failure occurs when loading and the breaking of cavities beneath the pavilion's base create a tensile zone under its foundation, leading to potential structural damage.

D. Unstable Zone Weight and Moment Calculation

Volume and Weight Calculation:

Formula: Saturated Unit Weight × Volume of Unstable Zone = Weight of Unstable Zone

Saturated Unit Weight: Approximately 2.20 – 2.30 t/m^3, Moment (Torque) Calculation:

Formula: Moment = 15 × Weight of Unstable Zone

E. Engineering Geological Mapping

According to the engineering geological map of the Niasar area, the upper part of the slope, located directly beneath the building, consists of impurities and intermixed marl with travertine. This section is highly unstable. Beneath this weak upper layer lies a zone of highly karstified travertine. This section exhibits partial instability due to extensive karstification, which creates voids, fractures, and irregularities within the rock mass. Further below, the dark-colored travertine layer is characterized by a lower degree of karstification and reduced impurity content. Compared to the upper sections, this part of the slope is more stable due to its stronger lithological properties and lower susceptibility to erosion or collapse.

The area is classified into different zones through both macro and micro zoning, based on the results obtained from the slope stabilization model, categorizing the slope as stable, unstable, or partially stable. The upper section, situated directly beneath the historical building, is identified as the most unstable. The middle section, characterized by karstification with caves and vugs, is considered partially unstable. In contrast, the lower section is relatively stable compared to the upper two layers. Micro zoning further refines these three primary zones into subclasses A, B, and C, representing subdivisions of the macro zoning. Given the model's need for cost-effectiveness, the stable lower section can be assigned a lower priority for implementing engineering measures.

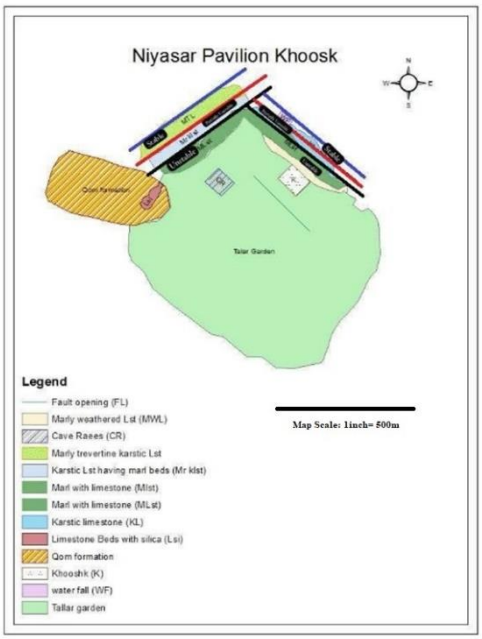

Fig. 28. Engineering geology map of Niasar water fall 1:5000 (Meybodi et al., 2026)

The slope stabilization model addresses uncertainties and limitations by employing a multi-faceted zonation approach and strategic prioritization. The macro and micro zoning of the slope into stable, partially stable, and unstable categories inherently acknowledges geological complexity, even when the underlying data is simplified, by treating different areas distinctly. This tiered zoning allows for a more nuanced representation than a single classification. Furthermore, the cost-effectiveness prioritization, which assigns a lower engineering priority to the stable lower section, implicitly manages uncertainties and potential data gaps. It suggests that while this area is likely stable based on current information, the assessment carries a degree of confidence that allows resources to be focused on the more critical, potentially unstable zones where interventions are most urgently needed. The inclusion of a "wet model" to account for pore water pressure, even with simplified hydrological assumptions, demonstrates an effort to incorporate critical environmental factors, with the understanding that this aspect may require further refinement. The distinction between macro and micro zoning also attempts to mitigate scale effects by providing both a broad overview and more localized detail. Therefore, rather than ignoring limitations, the model uses its zoning and prioritization framework as a practical mechanism to manage them, ensuring that the resulting classifications are actionable and resources are allocated efficiently, even when faced with incomplete data or simplified representations of natural phenomena.

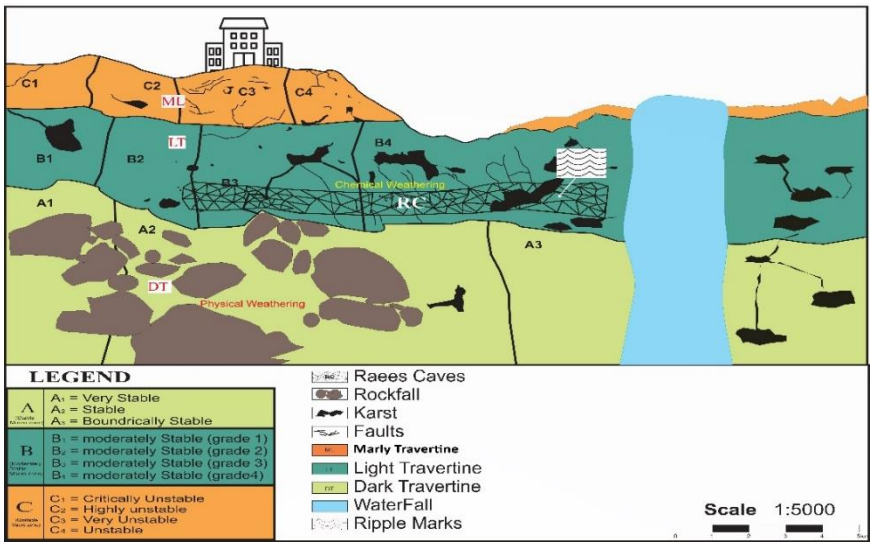

Fig. 29. The engineering geology rock zonation map of the Niasar slope area classifies the terrain according to the risk factors associated with potential rock failure

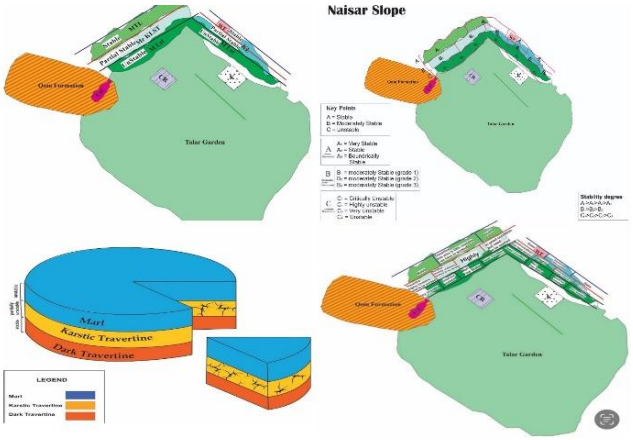

Fig. 30. Micro and macro-scale zoning of the Niasar slope, derived from numerical modeling data, specifically for the highly karstified region

XI. DISSCUSION AND CONCLUSION

Based on conducted studies and past incidents, it is confirmed that the Niasar slope is a dangerous area requiring stabilization through geotechnical methods. This paper evaluates the stability of the Niasar slope using a two-dimensional distinct element modeling approach with UDEC (Universal Distinct Element Code, Version 4.0). This numerical method is highly suitable for analyzing jointed rock masses, as it simulates interactions between discrete blocks along discontinuities. This capability allows for modeling complex failure mechanisms, such as sliding and toppling, which are common in unstable slopes (Stead et al., 2006). The simulation results reveal that in models without cracks, displacement remains negligible (0.02 mm), even with the application of horizontal acceleration. However, models incorporating cracks exhibit the highest total displacement in the second section, measuring 10 mm under a horizontal acceleration of 3, and 9 mm when the acceleration is zero. This highlights the significant impact of cracks on wall movement. Additionally, the combined effect of horizontal acceleration and downward force exacerbates displacement, ultimately leading to model collapse, as evidenced by corroborating stress-strain and X-Y displacement models. In the hydraulic model, where the mechanical model could not be applied due to UDEC software limitations, a slight movement of 0.01 mm was observed, confirming that groundwater also contributes to slope destabilization. Therefore, the interplay of these forces results in the destabilization of the entire area. Progressive damage in rock slopes may evolve over time before final failure, indicating that instability can develop gradually rather than as an instantaneous collapse (Jensen and Moore, 2023). Two major sets of discontinuities have contributed to the development of blocky or cube-shaped rock masses within the Kushk foundation bedrock. Rockfalls may occur progressively along the foundation wall as a result of the intersection of these vertical and horizontal discontinuity sets, as evidenced by the exposed wall conditions and previous rockfall events in the area. The horizontal discontinuity corresponds to the contact between lithological layers, specifically the boundary between the lower dark trevertine and the overlying karstified travertine. The vertical discontinuities are mainly tension joints formed by weathering and karst development. The intersection of these two discontinuity sets creates detached blocks with horizontal bases, separated from the underlying rock mass and therefore susceptible to sliding. These pre-existing instability conditions can become active under the influence of seepage water pressure within tension cracks, uplift pressure along the impermeable marl surface, and dynamic loading caused by seismic waves

impacting the back of the wall. The occurrence of a rockfall triggered by an earthquake approximately 30 years ago in this region further supports this mechanism.

Based on the UDEC 4.0 simulation outputs, the Niasar slope was classified into distinct stability zones. The upper section, directly beneath the historical building, was identified as the most unstable zone due to the presence of soft materials and impurities, showing significant modeled displacements. This is consistent with findings from other studies in which UDEC has been effective in identifying critical failure surfaces in complex rock slopes (Brideau et al., 2009; Havaej et al., 2016). The middle section, classified as partially stable, contains large vugs and caves, contributing to its instability. These cracks and vugs render the slope susceptible to self-instability. Micro-zoning played a crucial role here; to meet the demand for a cost-effective model, it identified zones requiring priority attention. In contrast, the lower section, which is more stable compared to the upper sections of the Niasar slope, exhibited a high factor of safety and minimal displacement, indicating stability under current conditions. Consequently, from a cost-effectiveness standpoint, this zone was assigned a lower priority for direct engineering intervention. This zonation framework, encompassing both macro-classes (stable, partially stable, unstable) and their corresponding micro-zones (subclasses A, B, and C), offers a robust foundation for prioritizing slope stabilization efforts. The application of the strength reduction technique within UDEC further validated the stability indices for each zone, a methodology consistent with established practices in rock slope analysis (Boon et al., 2014). Schmidt hammer and slake durability tests were conducted to evaluate the rock strength and its behavior under changing physical conditions. The results indicate that the rock mass possesses very low strength and is highly susceptible to weathering; when subjected to stress, the material can weather and erode at a significant rate (Haider et al., 2024). The unusual geotechnical behavior observed poses challenges for the application of conventional rock mass classification methods, such as the Rock Mass Rating (RMR) system or traditional Rock Quality Designation (RQD) derived from drilled core samples. These methods rely on intact core recovery and specific structural assessments, which are not feasible with such weak materials. Consequently, the input parameters for the slope model were selected based on values suggested by Hoek and Brown and other researchers, specifically tailored for analyzing highly karstified and weak rock masses. The findings from these studies offer critical guidance for geotechnical engineers involved in slope stabilization. Due to the weak and unstable nature of the rock mass, traditional methods like grouting or nailing alone are insufficient for the unstable zones. Effective stabilization of these areas requires a comprehensive approach combining techniques such as grouting, anchoring, geotextiles, nailing, and retaining walls. The zonation map facilitates a better understanding of specific ground conditions, enabling engineers to apply targeted stabilization methods appropriate for each distinct zone. This targeted strategy ensures that engineering solutions not only achieve stability but also preserve the original aesthetic and structural integrity of the slope.

References

Aghanabati, A. (2004). Geology of Iran. Geological Survey of Iran.

Boon, C. W., Houlsby, G. T., & Utili, S. (2014). A new rock slicing method based on linear programming. Rock Mechanics and Rock Engineering, 47(2), 621–639.

Brideau, M. A., Yan, M., & Stead, D. (2009). The role of tectonic damage and brittle rock fracture in the development of large rock slope failures. Geomorphology, 103(1), 30 49.

Coevolution of rock slope instability damage and resonance frequencies. (2023). Journal of Geophysical Research: Earth Surface, 128(11), e2023JF007305. https://doi.org/10.1029/2023JF007305

Ehsan, M., Anees, M. T., Bakar, A. F. B. A., & Ahmed, A. (2025). A review of geological and triggering factors influencing landslide susceptibility: Artificial intelligence-based trends in mapping and prediction. International Journal of Environmental Science and Technology, 22(16), 17347-17382.

Meybodi, E.E., Haider, H. and Akhtar, S. (2026). Electrical Survey Applications in Karstic Terrain (Resistivity & IP Survey); Cave Detection, Macro & Micro Rock Zonation for Rock Stability A Case Study of Naisar waterfall Kashan Iran. Journal of Analytical and Numerical Methods in Mining Engineering, 16(47), 17-26.

Meybodi, E.E., Hussain, S.K. (2022). The Karstic Geomorphology in The Dolomite of Drinjal Formation in Central Iran (Case Study Saddat Sirize Iron Mine). Earth Sciences Malaysia, 6(1): 11-14.

Meybodi, E.E., Hussain, S. K., Torabi-Kaveh, M., & Ali, S. (2022). Role of karstic features in instability of the wall of an open-pit mine (case study: Sadat Sirize Iron Mine, Iran). Carbonates and Evaporites, 37(3), 52.

Haider, H. , Akhtar, S. , Emami, E. , Masood, K. and Hussain, K. (2024). Manufacturing Of Cement And Petrography Of Its Raw Materials. Journal of Geomine, 2(2), 50-57.

Havaej, M., Coggan, J., Stead, D., & Elmo, D. (2016). A combined remote sensing–numerical modelling approach to the stability analysis of the 2012 Preonzo rock slope failure. Landslides, 13(5), 1243–1253.

Hoek, E., Brown, E. T. (1997). Practical estimates of rock mass strength. International Journal of Rock Mechanics and Mining Sciences, 34(8), 1165-1186.

Jensen, E. K., & Moore, J. R. (2023). Coevolution of rock slope instability damage and resonance frequencies from distinct-element modeling. Journal of Geophysical Research: Earth Surface, 128(11), e2023JF007305.

Li, J., Li, B., Wan, J., Gao, Y., Li, J., & Li, H. (2025). Hydrodynamic characteristics and failure mechanism of karst conduct flow on landslide under heavy rainfall. Geomatics, Natural Hazards and Risk, 16(1), 2584702.

Lukačić, H., Noël, F., Jaboyedoff, M., & Krkač, M. (2024). Impact of discontinuity data acquisition methods on rockfall susceptibility assessment using high-resolution 3D point cloud. Engineering geology, 340, 107677.

Marinos, P., & Hoek, E. (2000). GSI: A geologically friendly tool for rock mass strength estimation. Proceedings of GeoEng2000 Conference, 1422-1440

Schlumberger. (2011). Carbonate reservoir characterization: An integrated approach. Oilfield Review, 23(1), 4–17

Stead, D., Eberhardt, E., & Coggan, J. S. (2006). Developments in the characterization of complex rock slope deformation and failure using numerical modelling techniques. Engineering Geology, 83(1-3), 217–235.

Waltham, T., Bell, F. G., & Culshaw, M. G. (2005). Rocks, dissolution and karst. Sinkholes and Subsidence: Karst and Cavernous Rocks in Engineering and Construction, 1-23.